

CGIBNet: Bandwidth-constrained Communication with Graph Information Bottleneck in Multi-Agent Reinforcement Learning

Qi Tian, Kun Kuang, Baoxiang Wang, Furui Liu, and Fei Wu, *Senior Member, IEEE*

Abstract—Communication is one of the core components for cooperative multi-agent reinforcement learning (MARL). The communication bandwidth, in many real applications, is always subject to certain constraints. To improve communication efficiency, in this article, we propose to simultaneously optimize whom to communicate with and what to communicate for each agent in MARL. By initiating the communication between agents with a directed complete graph, we propose a novel communication model, named Communicative Graph Information Bottleneck Network (CGIBNet), to simultaneously compress the graph structure and the node information with the graph information bottleneck principle. The graph structure compression is designed to cut the redundant edges for determining whom to communicate with. The node information compression aims to address the problem of what to communicate via learning compact node representations. Moreover, CGIBNet is the first universal module for bandwidth-constrained communication, which can be applied to various training frameworks (*i.e.*, policy-based and value-based MARL frameworks) and communication modes (*i.e.*, single-round and multi-round communication). Extensive experiments are conducted in Traffic Control and StarCraft II environments. The results indicate that our method can achieve better performance in bandwidth-constrained settings compared with state-of-the-art algorithms, especially for large-scale multi-agent tasks.

Index Terms—multi-agent reinforcement learning, graph information bottleneck, bandwidth-constrained communication, multi-agent system.

I. INTRODUCTION

MULTI-AGENT reinforcement learning (MARL) has shown its powerful ability to cope with many complex decision-making tasks, such as sensor networks [1], traffic networks [2], strategy games [3]–[5] and swarm robotics [6]. In these scenarios, the communication mechanism is regarded as a promising way to improve team collaboration, as multiple agents can exchange their local observations or corresponding embeddings with each other during the execution phase to make a better joint decision. Therefore, a variety of works have been proposed in the field of multi-agent communication to improve the performance of MARL [7]–[16].

In real multi-agent systems, however, communication resources are usually limited. Under this setting, the key problem

Qi Tian, Kun Kuang and Fei Wu are with College of Computer Science and Technology, Zhejiang University, Hangzhou 310027, China. (email: tianqics, kunkuang, wufei@zju.edu.cn).

Baoxiang Wang is with School of Data Science, Chinese University of Hong Kong (Shenzhen), Shenzhen 518000, China. (email: bxwang@gmail.com).

Furui Liu is with Huawei Noah's Ark Lab, Huawei Technologies, Shenzhen 518000, China. (email: liufurui2@huawei.com).

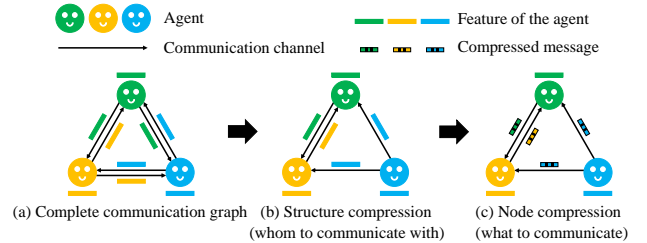


Fig. 1. An illustration of graph structure and node information compression in our CGIBNet. (a) A directed complete graph is proposed to model multi-agent communication in MARL. (b) Graph structure compression is designed for identifying whom to communicate with. (c) Node information compression is used to learn what to communicate.

is how to efficiently exploit the available bandwidth and reduce the redundant communication among multi-agents. One possible solution is to optimize whom to communicate with and what to communicate for each agent in MARL. In this article, we focus on the problem of bandwidth-constrained communication in MARL, which is with the following challenges: (1) **Whom to communicate with?** Each agent needs to identify the agents that are necessary to communicate with for a good teamwork and establish an efficient cooperation protocol among multiple agents; (2) **What to communicate?** Each agent needs to deliver a concise and compact message, otherwise one large message may deplete the whole communication resources.

Recently, many methods [17]–[22] have been proposed to address the above challenges, but they have the following shortcomings: 1) Existing methods only focus on one of the challenges. *e.g.*, [17]–[20] solve the first challenge, while [21], [22] solve the second. A seemingly straightforward idea is to combine these methods to simultaneously overcome both challenges. However, due to the lack of unified theoretical guidance and the compatibility problems of the methods, this combination can only achieve sub-optimal performance, as we will show in the experiments. 2) Many previous methods [18]–[21] need to learn an extra actor for message aggregation, hence are limited to policy-based MARL frameworks and cannot be applied to value-based MARL frameworks [23]. 3) All these methods are designed for single-round communication and cannot compress the communication bandwidth in multiple rounds of communication. Hence, it is of paramount importance to design a universal communication model that can simultaneously address the challenges of whom and what

to communicate, and can be applied to various training frameworks (*i.e.*, policy-based and value-based MARL frameworks) and communication modes (*i.e.*, single-round and multi-round communication).

To achieve this goal, in this article, we propose a novel and universal multi-agent communication model named Communicative Graph Information Bottleneck Network (CGIBNet). Specifically, we first model multi-agent communication with a directed complete graph as is shown in Figure 1(a). Then we derive two optimizable variational upper bounds based on the graph information bottleneck (GIB) principle and instantiate them into two regularizers to compress graph structure and node information. The graph structure compression regularizer is designed for addressing the challenge of whom to communicate with as is shown in Figure 1(b), by reducing the unnecessary communication channels between agents and maximally preserving information for decision-making. Moreover, in the setting of multi-round communication, this regularizer can also be used in each layer of the graph to reduce communication overhead in each communication round. The node information compression regularizer is designed for solving the problem of what to communicate as is shown in Figure 1(c), by learning compact node representations to reduce bandwidth occupancy. Since the structure learning of CGIBNet is modeled as a link prediction task [24] instead of an actor-based scheduler, our model is learned implicitly with downstream reinforcement learning tasks in an end-to-end manner, hence, can be easily applied to the existing MARL frameworks (*i.e.*, policy-based and value-based MARL) and communication models (*i.e.*, single-round and multi-round communication).

We summarize our contributions as follows:

- We investigate the problem of bandwidth-constrained communication in MARL by simultaneously considering with whom and what to communicate. We address this problem through the GIB principle and an optimization surrogate with rigorous theoretical guarantees.
- We propose a novel CGIBNet based on the GIB principle, to jointly compress the structure and node information of the communication graph for identifying with whom and what to communicate. CGIBNet is a universal module, which can be applied to various training frameworks (*i.e.*, policy-based and value-based MARL frameworks) and communication modes (*i.e.*, single-round and multi-round communication).
- Extensive experiments on both Traffic Control and StarCraft II datasets show that our proposed method outperforms the state-of-the-art algorithms, especially for those large-scale multi-agent systems.

II. RELATED WORK

MARL communication. Communication plays an important role in the MARL research since it can alleviate the non-stationary problem of multi-agent systems, thereby improving the group’s cooperation [23]. Recently, a variety of works have been proposed to explore communication protocols in MARL, such as improving the message aggregation mechanism [7]–[11], introducing memory modules [12], [13], learning world

dynamic models [14], [15], adjusting experience buffers [16], *etc.* However, all the above methods require each agent to receive the messages from all agents in each control cycle to take an action, which is not suitable for practical scenarios where communication bandwidth is limited. To efficiently utilize finite communication resources, the existing works reduce the communication burden from two points: 1) who to communicate with (structure information) and 2) what to communicate (node information).

For the first point, researchers introduce various gating mechanisms to reduce communication channels between agents. *e.g.*, IC3Net [18] models the gate by learning an extra actor, while G2A [17] achieves this goal through hard attention and combines with soft attention to improve its performance. However, IC3Net and G2A do not explicitly constrain or penalize the communication frequency, thus these methods still occupy a lot of communication overhead. SchedNet [19] and ETCNet [20] leverage actor-based weight generators to explicitly restrict bandwidth occupancy, thus these methods can save some communication channels. Unfortunately, all the existing methods have some application limitations. Specifically, IC3Net, SchedNet and ETCNet can only be applied to policy-based MARL frameworks. This is because they model communication scheduler as an actor μ and directly optimize the parameter θ of μ by policy gradient theorem [25], *i.e.*, $A\nabla_{\theta} \log \mu$, which is not feasible in value-based methods since there is no policy gradient theorem. For a similar reason, these methods can only achieve single-round communication, because recursive optimization gradient $A\nabla_{\theta}(\log \mu(\nabla_{\theta} \log \mu))$ in multiple rounds of communication does not conform to the policy gradient theorem. G2A is not limited by the training frameworks, however, this method can only be used for single-round communication since its message aggregation module (*i.e.*, BiLSTM [26]) is not compatible with the multi-round communication process.

For the second point, researchers introduce various regularizers to learn compact message representations. *e.g.*, NDQ [22] derives two regularizers based on mutual information to ensure the expressiveness and succinctness of the message. However, this method does not design a message aggregation module but uses fully connected communication, resulting in sub-optimal message representations and poor performance in some specific scenarios. *e.g.*, target communication is needed [10]. IMAC [21] is most relevant to our work since it also introduces the information bottleneck (IB) principle [27]. We emphasize the differences between our method and IMAC as follows: 1) Theory: The IB principle used by IMAC can only solve the problem of what to communicate (*i.e.*, compress message representations) for each agent, but has no theoretical guidance on who to communicate with (*i.e.*, reduce communication channels). However, we extend the IB principle to the graph information bottleneck (GIB) principle, which can simultaneously solve the above two problems under a unified framework. 2) Instantiation: Although IMAC claims that it can determine each agent is communicating to whom by learning a message aggregation module, we find this module cannot reduce communication channels between agents since it still uses the fully connected style. Therefore, no matter in theory

TABLE I
PROPERTIES OF DIFFERENT METHODS.

	Schedule structure information	Value-based framework	Policy-based framework	Theoretical guarantee	Compress structure information	Compress node information	Multi-round communication
IC3Net [18]	✓		✓				
G2A [17]	✓	✓	✓				
SchedNet [19]	✓		✓		✓		
ETCNet [20]	✓		✓	✓	✓		
NDQ [22]		✓	✓	✓		✓	
IMAC [21]	✓		✓	✓		✓	
CGIBNet (ours)	✓	✓	✓	✓	✓	✓	✓

or implementation, IMAC cannot reduce communication overhead in terms of who to communicate with. Furthermore, the message aggregation module of IMAC is modeled as an actor, which means that it has many usage restrictions similar to IC3Net, SchedNet and ETCNet. Different from these methods, we model the message scheduler as a link prediction task [24] in graph neural networks, which can be naturally combined with our deduced information-theoretic regularizer and achieve end-to-end training without the above application limitations.

For better comparison, we list the properties of different methods as shown in Table I. Note that the difference between ‘Schedule structure information’ and ‘Compress structure information’ is that the latter explicitly constrains or penalizes the redundant structural information.

Information bottleneck. Information bottleneck (IB), originally proposed for signal processing, tries to find a short code of the input signal but preserves maximum information of the code [28]. Alemi et al. [27] first introduce the IB into deep neural networks, then the IB is applied to various domains [29]–[31]. Recently, Wu et al. [32] extend the IB theory to the graph data to learn compact node representations, which can improve model robustness against adversarial examples [33]. However, they assume that the graph data satisfies the local-dependence assumption and the underlying graph is a static graph (*i.e.*, each layer of the graph structure is consistent and constant). Instead, we deal with a dynamic graph (*i.e.*, the structure of the communication graph is different at each timestep). Meanwhile, we assume the structure of the lower layer is based on the upper layer in multiple rounds of communication. These lead to the differences between our method and their method in terms of both theoretical derivation and instantiation.

III. PRELIMINARY

A. Dec-POMDP and cooperative MARL.

A fully cooperative multi-agent task can be described as a Decentralized Partially Observable Markov Decision Process (Dec-POMDP) [34] and defined as a tuple $\langle N, \mathcal{S}, \mathcal{A}, \mathcal{T}, \mathcal{R}, \mathcal{O}, \Omega, \gamma \rangle$, where N represents the number of agents. \mathcal{S} represents the true state space of the environment. At each timestep $t \in \mathcal{Z}^+$, each agent $i \in N \equiv \{1, \dots, n\}$ takes an action $a_i \in \mathcal{A}$, forming a joint action $\mathbf{a} \in \mathcal{A} \equiv \mathcal{A}^n$. Let $\mathcal{T}(s'|s, \mathbf{a}) : \mathcal{S} \times \mathcal{A} \rightarrow \mathcal{S}$ represents the state transition function. All agents share the global reward function $r(s, \mathbf{a}) :$

$\mathcal{S} \times \mathcal{A} \rightarrow \mathcal{R}$. Since we consider a partially observable setting, each agent receives an individual observation $o_i \in \Omega$ according to the observation function $\mathcal{O}(s, a) : \mathcal{S} \times \mathcal{A} \rightarrow \Omega$. $\gamma \in [0, 1)$ represents the discount factor. The current timestep superscript t is omitted for all variables if there is no ambiguity.

B. Policy-based and value-based MARL training frameworks.

1) *Policy-based MARL:* Independent actor-critic (IAC) [35] is the simplest multi-agent policy gradient method, which treats each agent as an independent learner. For each agent i , the main idea is to directly adjust the parameters θ_i of the actor policy π_i in order to maximize the objective by taking steps in the direction of its gradient. By the policy gradient theorem [25], the gradient of the objective is

$$\nabla_{\theta_i} \mathcal{L}_{MARL,i}^{IAC} = \mathbb{E}_{\pi_i} [A_i(o_i) \nabla_{\theta_i} \log \pi_i(a_i|o_i)], \quad (1)$$

where $\mathbb{E}_{\pi_i}[\cdot]$ represents the sampled training data produced by the current policy π_i . $A_i(o_i)$ represents the advantage function. However, the decision-making of each agent is influenced by the non-stationarity problem [36] in multi-agent systems, so the advantage function based on local information o_i may be estimated inaccurately. A reasonable alternative is the centralized advantage function $A_i(s)$ that incorporates global information s to alleviate this problem.

Further, to reuse historical data, importance sampling is applied in (1), as

$$\nabla_{\theta_i} \mathcal{L}_{MARL,i} = \mathbb{E}_{\pi_{i,\text{old}}} [\rho_i A_i(s) \nabla_{\theta_i} \log \pi_i(a_i|o_i)], \quad (2)$$

where $\mathbb{E}_{\pi_{i,\text{old}}}[\cdot]$ represents the sampled training data produced by the old policy $\pi_{i,\text{old}}$ and $\rho_i = \pi_i(o_i|a_i) / \pi_{i,\text{old}}(o_i|a_i)$ represents the importance weight to correct the bias. Unfortunately, (2) would lead to an excessively large policy update if without constraints. To penalize changes of policy and ensure the efficiency of importance sampling, Yu et al. [37] propose a multi-agent version of the clipped PPO [38]

$$\begin{aligned} \nabla_{\theta_i} \mathcal{L}_{MARL,i}^{MAPPO} &= \mathbb{E}_{\pi_{i,\text{old}}} [\min(\zeta_1, \zeta_2) \nabla_{\theta_i} \log \pi_i(a_i|o_i)] \\ \zeta_1 &= \rho_i A_i(s) \\ \zeta_2 &= \text{clip}(\rho_i, 1 - \epsilon, 1 + \epsilon) A_i(s), \end{aligned} \quad (3)$$

where ϵ is a hyperparameter to control the feasible range of the policy update. In this article, MAPPO will be used as one of the basic MARL frameworks for multi-agent communication.

2) *Value-based MARL:* Value decomposition is a popular technical line in the value-based MARL [23], among which

QMIX [39] is a representative work. It assumes that the total action-value function Q_{tot} can be decomposed into individual action-value functions Q_i , which satisfies the following relation

$$\operatorname{argmax}_{\mathbf{a}} Q_{tot}(s, \mathbf{a}) = \begin{pmatrix} \operatorname{argmax}_{a_1} Q_1(o_1, a_1) \\ \vdots \\ \operatorname{argmax}_{a_n} Q_n(o_n, a_n) \end{pmatrix}. \quad (4)$$

Further, the authors observe this representation can be generalized to the larger family of monotonic functions that are also sufficient but not necessary to satisfy (4). Monotonicity can be enforced through the constraint

$$\frac{\partial Q_{tot}}{\partial Q_i} \geq 0, \quad \forall i \in N. \quad (5)$$

QMIX uses a mixer hypernetwork [40] to implement this constraint. Then all network parameters can be optimized by a Q -learning style [41] loss function as follows

$$\mathcal{L}_{MARRL}^{QMIX} = (y_{tot} - Q_{tot}(s, Q_1(o_1, a_1), \dots, Q_n(o_n, a_n)))^2, \quad (6)$$

where $y_{tot} = r + \gamma \max_{\mathbf{a}'} Q_{tot}^-(s', Q_1^-(o_1', a_1'), \dots)$ and $(\cdot)^-$ represents target networks. $(\cdot)'$ represents the variable at the next timestep. In this article, we choose QMIX as one MARL framework for the evaluation of communication modules.

C. MARL with communication mechanism.

In communication settings, multiple agents can transmit messages to each other for better collaboration. Therefore, the policy π_i in (3) and the individual action-value function Q_i in (6) can be rewritten as

$$\begin{aligned} \text{Policy-based MARL (MAPPO): } & \pi_i(a_i | o_i, \mathbf{m}_{-i}) \\ \text{Value-based MARL (QMIX): } & Q_i(o_i, a_i, \mathbf{m}_{-i}), \end{aligned} \quad (7)$$

where $\mathbf{m}_{-i} = [m_1, \dots, m_{i-1}, m_{i+1}, \dots, m_N]$ represents the total messages that agent i receives from its teammates, and each individual message m_j ($j \in 1, \dots, N$ and $j \neq i$) is usually obtained by dimensionality reduction mapping of local observations $m_j = \Psi(o_j)$. In this article, we focus on bandwidth-constrained settings, which means that each agent i cannot obtain all messages from other agents and can only pick some important ones.

IV. METHODOLOGY

In this section, we first illustrate the problem definition in this article. Then we detail the GIB principle in MARL communication to show its mechanism of saving communication resources. Based on the GIB principle, we propose a novel communication model (CGIBNet). Finally, we introduce the method to plug CGIBNet into both policy-based and value-based frameworks.

A. Problem definition

Our work focuses on how to learn a communication model to determine what messages to send and whom to address them in bandwidth-restricted settings. In order to simultaneously solve these two problems under a unified framework, we first

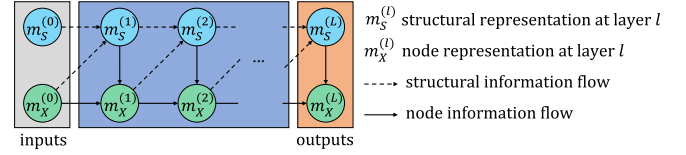


Fig. 2. Information flow in the communication graph

model multi-agent communication as a graph, where nodes represent agents and edges represent communication channels between agents. Therefore, the communication process can be regarded as the message passing [42] of each node information under the current graph structure. Without loss of generality, we assume that there are L rounds of communication between agents [10] so that the communication graph has L layers. Then the structural representation $m_S^{(l)}$ and the node representation $m_X^{(l)}$ at the l -th layer can be denoted as

$$\begin{aligned} m_S^{(l)} &= \{m_{S,e}^{(l)}, m_{S,e}^{(l)} \in \{0, 1\} \text{ and } e \in \mathcal{E}\} \\ m_X^{(l)} &= \{m_{X,v}^{(l)}, m_{X,v}^{(l)} \in \mathbb{R}^d \text{ and } v \in \mathcal{V}\}, \end{aligned} \quad (8)$$

where \mathcal{E} and \mathcal{V} indicate the valid edge set and the node set at the l -th layer, 0 and 1 indicate the existence of the corresponding edge, d indicates the dimension of the node representation or the number of bits of each node message [22]. Under the above definition, reducing the bandwidth of multi-agent communication is equivalent to compressing the flow of structural information and node information in the communication graph. The former leads to fewer edge connections and the latter means that fewer bits can be used to express the whole node information.

B. GIB principle in MARL communication

Inspired by the information bottleneck (IB) principle [27], which is an information-theoretic principle that extracts the minimal sufficient representation for the target task, we extend it to the graph information bottleneck (GIB) principle in multi-agent communication. Specifically, we introduce two GIB-based criteria to compress the information flow over graph structures.

The first (minimum) criterion is to respectively constrain the structure-level mutual information $I(m_S^{(l-1)}; m_S^{(l)})$ and the node-level mutual information $I(m_X^{(l-1)}; m_X^{(l)})$ between adjacent layers to I_S and I_X . This can obtain concise and compact information flow to reduce communication consumption. In detail, different from [32], they assume that each layer of the graph structure is consistent and constant, while we consider that the lower structure representation is related to the upper structure and node representation as is shown in Figure 2. Thus we rewrite the structure-level and node-level mutual information and denote them as structural information bottleneck $SIB^{(l)}$ and node information bottleneck $XIB^{(l)}$, respectively:

$$\begin{aligned} SIB^{(l)} &= I(m_S^{(l-1)}, m_X^{(l-1)}; m_S^{(l)}) < I_S \\ XIB^{(l)} &= I(m_X^{(l-1)}, m_S^{(l)}; m_X^{(l)}) < I_X. \end{aligned} \quad (9)$$

The second (sufficiency) criterion is to maximize the mutual information between all graph representations and the MARL target to preserve task-related information. Since the communication model is jointly trained with other models, it can be achieved by minimizing the MARL task loss.

According to the above analysis, we formulate the GIB principle in bandwidth-limited communication tasks as

$$\begin{aligned} & \min \mathcal{L}_{MARL} \\ \text{s.t. } & SIB^{(l)} < I_S \text{ and } XIB^{(l)} < I_X, \forall l \in L, \end{aligned} \quad (10)$$

where $\mathcal{L}_{MARL} \in \{\mathcal{L}_{MARL}^{MAPPO}, \mathcal{L}_{MARL}^{QMLX}\}$ represents the target task loss, I_S and I_X limit the amount of information for structural representations and node representations to decrease bandwidth usage.

Since (10) is hard to solve, we use the Lagrangian function to relax it into an unconstrained optimization problem

$$\min \mathcal{L}_{MARL} + \beta_S \sum_{l=1}^L SIB^{(l)} + \beta_X \sum_{l=1}^L XIB^{(l)}, \quad (11)$$

where β_S and β_X represent the Lagrangian multipliers that control the compression strength in the optimization. We ignore the terms $-\sum_{l=1}^L \beta_S I_S$ and $-\sum_{l=1}^L \beta_X I_X$ because we treat β_S and β_X as constants in practice, referring to previous famous IB literature [27]. It is notoriously hard to directly optimize $SIB^{(l)}$ and $XIB^{(l)}$ due to the intractability of the mutual information terms. Thus we first derive the variational upper bound of $SIB^{(l)}$ as follows

$$\begin{aligned} SIB^{(l)} &= I(m_S^{(l-1)}, m_X^{(l-1)}; m_S^{(l)}) \\ &= \mathbb{E}_{p(m_S^{(l-1)}, m_X^{(l-1)}, m_S^{(l)})} \log \left(\frac{p(m_S^{(l-1)}, m_X^{(l-1)}, m_S^{(l)})}{p(m_S^{(l-1)}, m_X^{(l-1)}) p(m_S^{(l)})} \right) \\ &= \mathbb{E}_{p(m_S^{(l-1)}, m_X^{(l-1)}, m_S^{(l)})} \log \left(\frac{p(m_S^{(l)} | m_S^{(l-1)}, m_X^{(l-1)})}{p(m_S^{(l)})} \right) \\ &= \mathbb{E}_{p(m_S^{(l-1)}, m_X^{(l-1)}, m_S^{(l)})} \log p(m_S^{(l)} | m_S^{(l-1)}, m_X^{(l-1)}) \\ &\quad - \mathbb{E}_{p(m_S^{(l-1)}, m_X^{(l-1)}, m_S^{(l)})} \log p(m_S^{(l)}) \\ &= \mathbb{E}_{p(m_S^{(l-1)}, m_X^{(l-1)}, m_S^{(l)})} \log p(m_S^{(l)} | m_S^{(l-1)}, m_X^{(l-1)}) \\ &\quad - \mathbb{E}_{p(m_S^{(l)})} \log p(m_S^{(l)}). \end{aligned} \quad (12)$$

However, it is difficult to compute the marginal distribution $p(m_S^{(l)})$, so let $r(m_S^{(l)})$ be a variational approximation to this marginal. Then we have

$$\begin{aligned} D_{KL}(p(m_S^{(l)}) || r(m_S^{(l)})) &\geq 0 \\ -\mathbb{E}_{p(m_S^{(l)})} \log p(m_S^{(l)}) &\leq -\mathbb{E}_{p(m_S^{(l)})} \log r(m_S^{(l)}), \end{aligned} \quad (13)$$

where $D_{KL}(\cdot || \cdot)$ represents Kullback-Leibler (KL) divergence [43]. Substituting (13) into (12), we have

$$\begin{aligned} & SIB^{(l)} \\ & \leq \mathbb{E}_{p(m_S^{(l-1)}, m_X^{(l-1)}, m_S^{(l)})} \log p(m_S^{(l)} | m_S^{(l-1)}, m_X^{(l-1)}) \\ & \quad - \mathbb{E}_{p(m_S^{(l)})} \log r(m_S^{(l)}) \\ & \leq \mathbb{E}_{p(m_S^{(l-1)}, m_X^{(l-1)}, m_S^{(l)})} \log \left(\frac{p(m_S^{(l)} | m_S^{(l-1)}, m_X^{(l-1)})}{r(m_S^{(l)})} \right). \end{aligned} \quad (14)$$

Thus the upper bound of $SIB^{(l)}$ can be written as

$$\begin{aligned} \widehat{SIB}^{(l)} &= \mathbb{E}_{p_{S,X,S}} \left[\log \frac{p(m_S^{(l)} | m_S^{(l-1)}, m_X^{(l-1)})}{r(m_S^{(l)})} \right] \\ &= \mathbb{E}_{p_{S,X}} D_{KL}(p(m_S^{(l)} | m_S^{(l-1)}, m_X^{(l-1)}) || r(m_S^{(l)})), \end{aligned} \quad (15)$$

where $p_{S,X,S}$ represents $p(m_S^{(l-1)}, m_X^{(l-1)}, m_S^{(l)})$ and $p_{S,X}$ represents $p(m_S^{(l-1)}, m_X^{(l-1)})$. Similarly, we can get the upper bound of $XIB^{(l)}$ by replacing the above variables $m_S^{(l-1)} \rightarrow m_S^{(l)}$ and $m_S^{(l)} \rightarrow m_X^{(l)}$, then we have

$$\begin{aligned} \widehat{XIB}^{(l)} &= \mathbb{E}_{p_{X,S,X}} \left[\log \frac{p(m_X^{(l)} | m_X^{(l-1)}, m_S^{(l)})}{r(m_X^{(l)})} \right] \\ &= \mathbb{E}_{p_{X,S}} D_{KL}(p(m_X^{(l)} | m_X^{(l-1)}, m_S^{(l)}) || r(m_X^{(l)})), \end{aligned} \quad (16)$$

where $p_{X,S,X}$ represents $p(m_X^{(l-1)}, m_S^{(l)}, m_X^{(l)})$ and $p_{X,S}$ represents $p(m_X^{(l-1)}, m_S^{(l)})$. Substituting (15) and (16) into (11) obtains a GIB-based optimization surrogate of communication.

In order to calculate (15) in practice, we need to sample $m_S^{(l-1)}$ and $m_X^{(l-1)}$ at the $(l-1)$ -th layer to calculate the valid structural representation $m_S^{(l)}$ at the l -th layer. After $m_S^{(l)}$ is obtained, the empirical estimation of $\widehat{SIB}^{(l)}$ is denoted as

$$\overline{SIB}^{(l)} = \sum_{e \in \mathcal{E}} D_{KL}(p_e^{(l)}(m_S^{(l)} | m_X^{(l-1)}, m_S^{(l-1)}) || r(m_S^{(l)})), \quad (17)$$

where \mathcal{E} represents the valid edge set at the l -th layer. $r(m_S^{(l)})$ is known as the prior structure distribution. Similarly, we can get the empirical estimation of (16) by replacing the above variables $m_S^{(l-1)} \rightarrow m_S^{(l)}$ and $m_S^{(l)} \rightarrow m_X^{(l)}$, then we have

$$\overline{XIB}^{(l)} = \sum_{v \in \mathcal{V}} D_{KL}(p_v^{(l)}(m_X^{(l)} | m_X^{(l-1)}, m_S^{(l)}) || r(m_X^{(l)})), \quad (18)$$

where \mathcal{V} represents the valid node set at the l -th layer and $r(m_X^{(l)})$ represents the prior node distribution.

C. Instantiating the GIB principle as CGIBNet

After the above efforts, we obtain two information-theoretic regularizers based on the GIB principle, *i.e.*, (17) and (18). As is shown in Figure 3(a), we instantiate them as a novel communication model, named Communicative Graph Information

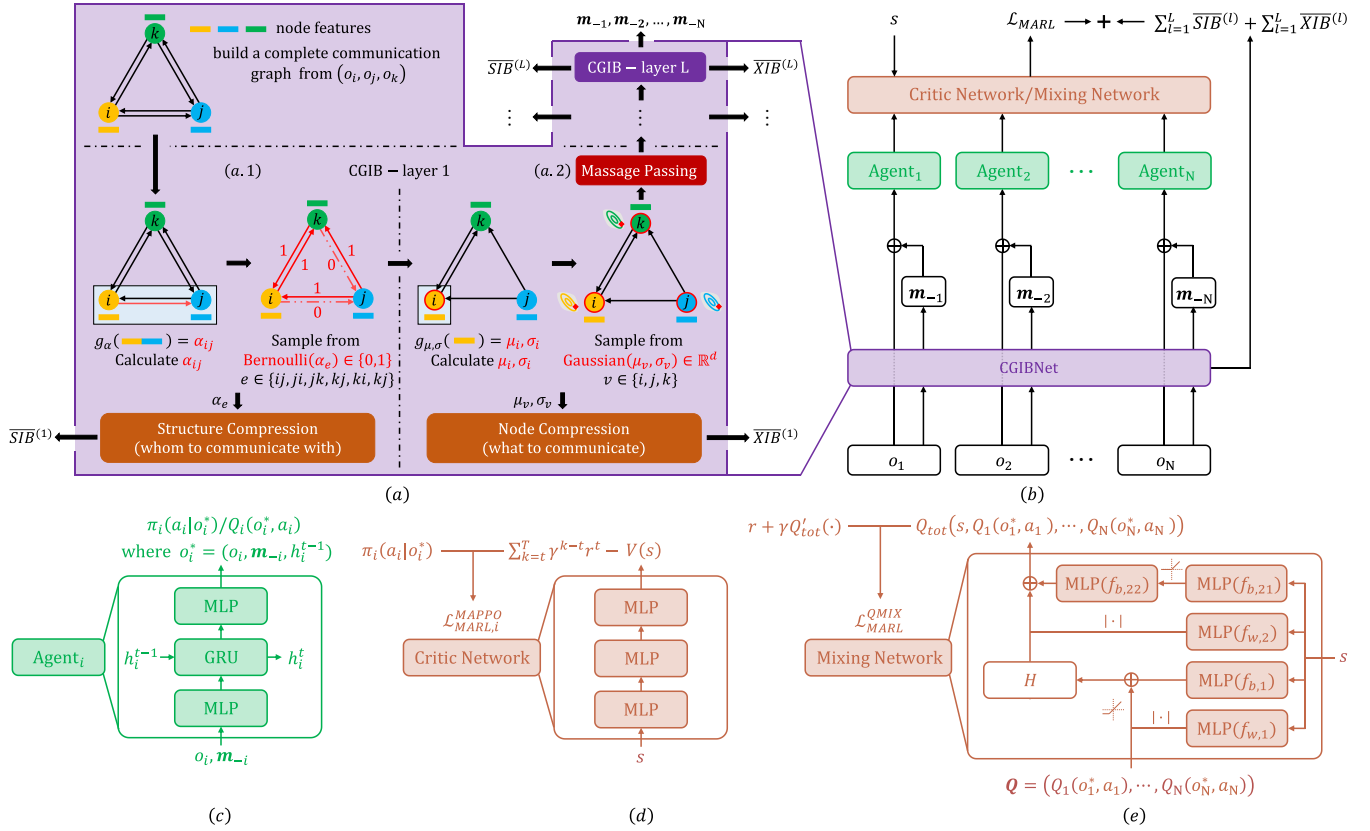


Fig. 3. Overall framework of our method. (a) CGIBNet, where (a.1) represents structure compression and (a.2) represents node compression. (b) overall training pipeline. (c) agent network. (d) critic network in policy-based MARL. (e) mixing network in value-based MARL.

Bottleneck Network (CGIBNet), which can simultaneously compress the structure and node information to solve the problem of with whom and what to communicate in bandwidth-limited communication.

Structure compression learning. In order to calculate $\overline{SIB}^{(l)}$ in (17) for structural compression, we first focus on the instantiation of $p_e^{(l)}(\cdot)$. Specifically, assuming that $m_{X,i}^{(l-1)} \in \mathbb{R}^d$ and $m_{X,j}^{(l-1)} \in \mathbb{R}^d$ are the node representations of node i and node j at the $(l-1)$ -th layer. We also suppose the structural representation $m_{S,ij}^{(l)} \in \{0, 1\}$ between these two nodes satisfies a Bernoulli distribution. With these assumptions, as is shown in Figure 3(a.1), we can calculate the parameter $\alpha_{ij}^{(l)}$ of Bernoulli distribution through a link prediction task [24]

$$\begin{aligned} & g_\alpha(m_{X,i}^{(l-1)}, m_{X,j}^{(l-1)}) \\ &= \text{sigmoid}(g_c(m_{X,i}^{(l-1)}, m_{X,j}^{(l-1)})) \\ &= \alpha_{ij}^{(l)}, \end{aligned} \quad (19)$$

where the sigmoid function constrains the output of the link prediction model g_c to the valid range $(0, 1)$. However, it is difficult to back-propagate the gradients if we directly sample $m_{S,ij}^{(l)}$ from $\text{Bernoulli}(\alpha_{ij}^{(l)})$. Hence we introduce a relaxed Bernoulli distribution, similar to [44], to solve it, as

$$m_{S,ij}^{(l)} \stackrel{\text{iid}}{\sim} \text{RelaxedBernoulli}(\alpha_{ij}^{(l)}, \tau), \quad (20)$$

where $\tau \in (0, \infty)$ is the temperature factor that controls the approximation. When τ is close to 0, $m_{S,ij}^{(l)}$ is approximately sampled from the set $\{0, 1\}$.

In the forward stage, the structural representation $m_S^{(l)}$ at the l -th layer can be obtained by repeating the process for all valid edges, as is shown in Figure 3(a.1). In the compression stage, the prior structure distribution $r(m_S^{(l)})$ in (17) is set to $\text{Bernoulli}(0.5)$ as an uninformative prior. Then incorporating (17) into (11) indicates that the structure representation can be compressed by minimizing the KL divergence between the posterior distribution $p_e^{(l)}(\cdot)$ and the prior distribution $r(m_S^{(l)})$.

Node compression learning. Following previous IB methods [27], [31], we present node embedding as a Gaussian random variable and use the reparameterization trick [45] to tackle the gradient blocking problem. That is, the node message at the $(l-1)$ -th layer can be obtained as

$$\begin{aligned} \epsilon & \stackrel{\text{iid}}{\sim} \text{Gaussian}(0, I) \\ m_{X,v}^{(l-1)} &= \mu_v^{(l-1)} \odot \epsilon + \sigma_v^{(l-1)}, \end{aligned} \quad (21)$$

where \odot represents the Hadamard product [46]. ϵ is sampled from $\text{Gaussian}(0, I)$. The mean $\mu_v^{(l-1)} \in \mathbb{R}^d$ and the variance $\sigma_v^{(l-1)} \in \mathbb{R}^d$ are obtained by the neural network $g_{\mu, \sigma}$ (Figure 3(a.2)), and d presents the number of bits. Since $m_S^{(l)}$ has been calculated in the structure learning stage, we can aggregate the information of $m_X^{(l-1)}$ through message passing. Specifically,

assuming that node i at the l -th layer needs to receive messages from node j and node k according to $m_S^{(l)}$. Then we have

$$g_m(m_{X,i}^{(l-1)}, m_{X,j}^{(l-1)}, m_{X,k}^{(l-1)}) = m_{X,aggre,i}^{(l)}, \quad (22)$$

where $m_{X,aggre,i}^{(l)}$ is used as the output of this layer. In the node compression stage, we set the prior node distribution $r(m_X^{(l)})$ to $\text{Gaussian}(0, I)$ as is in the previous work [27]. Then it amounts to minimize the current node information bottleneck of each node message to achieve node compression by (18). See Algorithm 1 for the pseudo-code of CGIBNet.

Drop message bits. Despite that all bits are maintained during the training process, we desire to discard some of them to satisfy the bandwidth constraints. An important observation is that the node information bottleneck of each message bit represents the amount of task-related information. Specifically, each bit (or dimension) b of all messages is optimized by

$$\min_b \sum \mathcal{L}_{MARL,b} + D_{KL}(\text{Gaussian}(\mu_b, \sigma_b) || \text{Gaussian}(0, I)). \quad (23)$$

We can find $\mathcal{L}_{MARL,b}$ and D_{KL} term is a trade-off. Assuming that the current node information bottleneck (*i.e.*, D_{KL} term) of all node bits is 0 after optimization, it means that the posterior Gaussian distribution of all bits is equal to the prior Gaussian distribution $\text{Gaussian}(0, I)$. Since there is no difference between these bits, they do not carry any useful information and $\mathcal{L}_{MARL,b}$ would not be small in the communication task. On the contrary, if the current node information bottleneck of one particular bit is large while the other bits are 0, it means that this bit is constrained by \mathcal{L}_{MARL} and carries most of the task-related information. Therefore, we can rank all bits according to their node information bottleneck, such that bits with the smallest amount of information are discarded after the training process.

D. Apply CGIBNet to MARL training frameworks

Since CGIBNet does not rely on the actor-based scheduler, it can be plugged into both policy-based and value-based MARL frameworks as is shown in Figure 3(b).

1) *Policy-based MARL (MAPPO)*: in this training framework, Agent $_i$ in Figure 3(b) represents individual policy π_i . It contains the memory cell GRU [47] to facilitate learning over longer timescales, as is shown in Figure 3(c). To simplify the expression, we combine the local observation o_i , received messages \mathbf{m}_{-i} and historical memory representation h_i^{t-1} as the generalized local observation $o_i^* = (o_i, \mathbf{m}_{-i}, h_i^{t-1})$. Then the decision-making of agent i can be denoted as $\pi_i(a_i | o_i^*)$.

The training policy gradient of each agent i refers to (3). In the implementation, as is shown in Figure 3(d), we choose Monte Carlo return with baseline $\sum_{k=t}^T \gamma^{k-t} r^k - V(s)$ as the advantage function $A_i(s)$, thus (3) can be rewritten as

$$\begin{aligned} \nabla_{\theta_i} \mathcal{L}_{MARL,i}^{MAPPO} &= \mathbb{E}_{\pi_{i,old}}[(\min(\zeta_1, \zeta_2) + \mathcal{G}) \nabla_{\theta_i} \log \pi_i(a_i | o_i^*)] \\ \zeta_1 &= \rho_i \left(\sum_{k=t}^T \gamma^{k-t} r^k - V(s) \right) \\ \zeta_2 &= \text{clip}(\rho_i, 1 - \epsilon, 1 + \epsilon) \left(\sum_{k=t}^T \gamma^{k-t} r^k - V(s) \right) \\ \mathcal{G} &= \beta_S \sum_{l=1}^L \overline{SIB}^{(l)} + \beta_X \sum_{l=1}^L \overline{XIB}^{(l)}, \end{aligned} \quad (24)$$

Algorithm 1: CGIBNet for MARL communication

Input: Observation (o_1, \dots, o_N) , edge network g_α , node network $g_{\mu, \sigma}$, aggregation network g_m , alive mask S , communication round L , temperature factor τ

- 1: Initialize the edge set $\mathcal{E} = \{m_{S,ij} = 1, 1 \leq i, j \leq N\}$, the node set $\mathcal{V} = \{m_{X,i} = \alpha_i, 1 \leq i \leq N\}$, $\overline{SIB} = \overline{XIB} = 0$
- 2: **for** $l = 1, 2, \dots, L$ **do**
- 3: According to S , if any agent i dies, set $m_{X,i} = \emptyset$, $m_{S,ik} = 0$, $m_{S,ki} = 0$ ($1 \leq k \leq N$)
- 4: **for** $m_{S,ij} \in \mathcal{E}$ **do**
- 5: **if** $m_{S,ij} = 1$ **then**
- 6: Calculate $\alpha_{ij} = g_\alpha(m_{X,i}, m_{X,j})$
- 7: Use α_{ij} to calculate \overline{SIB}_{ij} according to (17)
- 8: Calculate $\overline{SIB} = \overline{SIB} + \overline{SIB}_{ij}$
- 9: Sample new $m_{S,ij}$ according to (20)
- 10: **end if**
- 11: **end for**
- 12: **for** $m_{X,i} \in \mathcal{V}$ **do**
- 13: **if** $m_{X,i} \neq \emptyset$ **then**
- 14: Calculate $\mu_i, \sigma_i = g_{\mu, \sigma}(m_{X,i})$
- 15: Use μ_i, σ_i to calculate \overline{XIB}_i according to (18)
- 16: Calculate $\overline{XIB} = \overline{XIB} + \overline{XIB}_i$
- 17: Sample new $m_{X,i}$ according to (21)
- 18: **end if**
- 19: **end for**
- 20: **for** $m_{X,i} \in \mathcal{V}$ **do**
- 21: Concatenate all messages
 $M = \text{concat}(m_{X,1}, \dots, m_{X,N})$
- 22: Mask out the corresponding positions that do not send messages to agent i ($m_{S,ki} = 0$, ($1 \leq k \leq N$)) in M
- 23: Aggregate messages sent to agent i : $m_{X,i} = g_m(M)$
- 24: **end for**
- 25: **end for**
- 26: Assign $(\mathbf{m}_{-1}, \mathbf{m}_{-2}, \dots, \mathbf{m}_{-N}) = (m_{X,1}, m_{X,2}, \dots, m_{X,N})$
- 27: **return** $(\mathbf{m}_{-1}, \mathbf{m}_{-2}, \dots, \mathbf{m}_{-N}), \overline{SIB}, \overline{XIB}$

where γ represents the discount factor. T represents the terminal timestep. $V(s)$ represents the centralized value function, which is optimized by minimizing mean square error (MSE)

$$\mathcal{L}_{MARL,V}^{MAPPO} = \left(\sum_{k=t}^T \gamma^{k-t} r^k - V(s) \right)^2. \quad (25)$$

2) *Value-based MARL (QMIX)*: in this training framework, Agent $_i$ in Figure 3(b) represents individual action-value function $Q_i(o_i^*, a_i)$ and its network backbone is consistent with the above $\pi_i(a_i | o_i^*)$, as is shown in Figure 3(c).

To ensure the monotonic relation between total action-value function Q_{tot} and Q_i in (5) during training, the mixer hypernetwork is used as shown in Figure 3(e). Its key point is to restrict the weights (but not the biases) of the hybrid network to be non-negative, so that the mixing network can approximate any monotonic function arbitrarily closely [48]. Formally, $Q_{tot}(s, Q_1(o_1^*, a_1), \dots)$ can be calculated by

$$\begin{aligned} \mathbf{Q} &= (Q_1(o_1^*, a_1), \dots, Q_N(o_N^*, a_N)) \\ H &= \text{ELU}(\mathbf{Q} \cdot \text{abs}(f_{w,1}(s))) + f_{b,1}(s) \\ Q_{tot} &= H \cdot \text{abs}(f_{w,2}(s)) + f_{b,22}(\text{ReLU}(f_{b,21}(s))), \end{aligned} \quad (26)$$

where $f_{w,\cdot}(\cdot)$ and $f_{b,\cdot}(\cdot)$ represents the hyper weight networks and hyper bias networks (Figure 3(e)), respectively. abs represents absolute value operator. ELU represents exponential linear unit [49]. ReLU represents rectified linear unit [50].

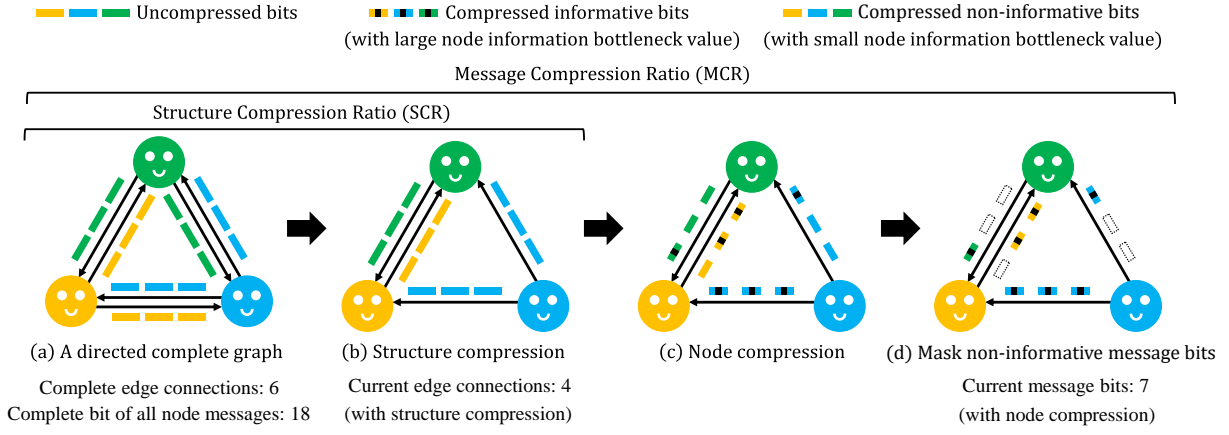


Fig. 4. Schematic diagram of calculation of SCR and MCR: $SCR = (6 - 4)/6 = 33.33\%$ and $MCR = (18 - 7)/18 = 61.11\%$.

Combined with our GIB-based regularizers, the loss of QMIX in (6) can be rewritten as

$$\begin{aligned} \mathcal{L}_{MARL}^{QMIX} &= (y_{tot} - Q_{tot}(s, Q_1(o_1^*, a_1), \dots))^2 + \mathcal{G} \\ \mathcal{G} &= \beta_S \sum_{l=1}^L \overline{SIB}^{(l)} + \beta_X \sum_{l=1}^L \overline{XIB}^{(l)}, \end{aligned} \quad (27)$$

where $y_{tot} = r + \gamma \max_{\alpha'} Q_{tot}^-(s', Q_1^-(o_1^*, a_1'), \dots)$.

V. EXPERIMENTS

In this section, we first introduce two metrics to measure bandwidth compression. Then we evaluate CGIBNet in two environments with bandwidth-constrained communication. The first one is Traffic Control, where we use a policy-based MARL framework (*i.e.*, MAPPO) for training. The second is the StarCraft II [51], where we use a value-based MARL framework (*i.e.*, QMIX) for training.

A. Evaluation Metric

Structure Compression Ratio (SCR). This metric refers to [19]. It focuses on the density of edge connections in the communication graph and assumes the message bits transmitted by each edge are consistent. Formally, let $N_{e,complete}$ and $N_{e,compressed}$ denote the number of edges of the communication graph structure without and with structure compression. Then, SCR is defined as

$$SCR = \frac{N_{e,complete} - N_{e,compressed}}{N_{e,complete}} \times 100\%. \quad (28)$$

For example, as is shown in Figure 4(b), there are 4 edge connections in the communication graph after structure compression, thus $SCR = (6 - 4)/6 = 33.33\%$.

Message Compression Ratio (MCR). This metric refers to [22]. It focuses on the message bits in the communication graph. The insight behind MCR is that the length of the message sent by each agent should be adaptive and various in different situations, and few node message bits can compress sufficient information for effective communication. However, the agent network requires the input of fixed-length messages. Therefore, we introduce a binary mask for each message bit to simulate controllable limited bandwidth. Formally, let

$N_{m,complete}$ denotes the message bits without compression and $N_{m,compressed}$ denotes the unmasked message bits with compression. Then, MCR is defined as

$$MCR = \frac{N_{m,complete} - N_{m,compressed}}{N_{m,complete}} \times 100\%. \quad (29)$$

We can find MCR can cover all cases of SCR according to their definition, thus MCR can reflect the degree of both structure and node compression. In practice, the masking strategy is based on the importance of each message bit. For methods that include node compression (*e.g.*, NDQ, IMAC, CGIBNet), we sort all message distributions in ascending order according to their current node information bottleneck, and mask them accordingly. *e.g.*, as is shown in Figure 4(d), the non-informative bits are masked first when the communication bandwidth is constrained. In this case, $MCR = (18 - 7)/18 = 61.11\%$. For the attention-based method (*e.g.*, G2A), we mask their message bits according to attention weights. For other methods, we mask their message bits according to their absolute value.

B. Traffic Control

Environment description. As is shown in Figure 5, each car is modeled as an agent, and they should learn a good cooperative policy to ensure that they can quickly pass through the junction with as few collisions as possible. The collision only affects the reward of the corresponding agent without changing the environment simulation. At the start of the episode, each car needs to randomly initialize a starting position near the entrance (*i.e.*, the highlighted area in Figure 5(a)) and randomly select one of the two possible routes. The termination condition of the environment is that all cars exit the junction or exceed the maximum timestep (20, 40, 60 for easy, medium and hard maps respectively). For each car, the local observation contains its location (*i.e.*, the one-hot value corresponding to the X-Y number in Figure 5(a)) and assigned route id. The action is a discrete number $a \in \{0, 1\}$, where 0 represents stop and 1 represents move one step forward. The reward consists of three parts: timestep penalty $r_{tp,i} = -1$, collision penalty $r_{cp,i} = -100$ and exit bonus $r_{eb,i} = 30$. Thus the shared total reward at timestep t is

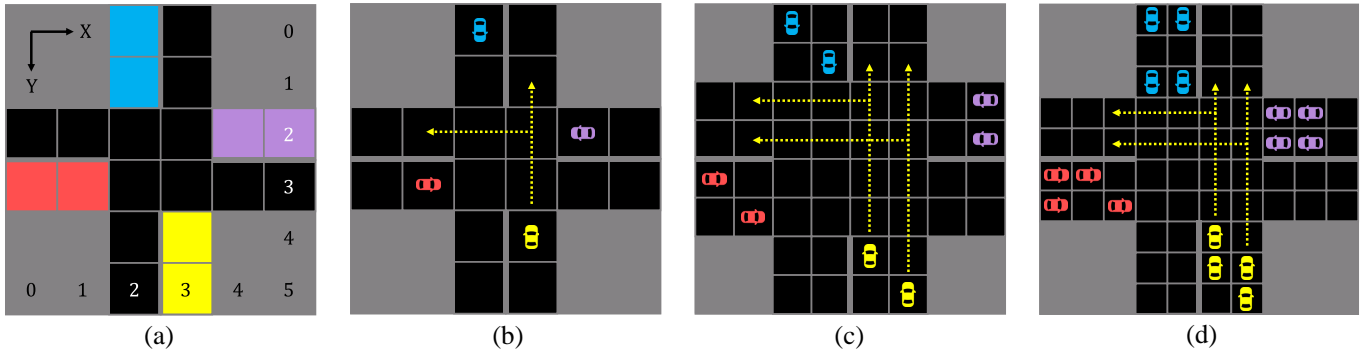


Fig. 5. Traffic control environment. (a) Initialization position (highlighted area) and local observation encoding (one-hot value corresponding to the X-Y number) in the easy map. (b) easy map (4 cars). (c) medium map (8 cars). (d) hard map (16 cars).

TABLE II
EXPERIMENTAL RESULTS IN DIFFERENT RESTRICTIONS ON TRAFFIC CONTROL.

Map	Easy						
	SCR	R under the left SCR	R under MCR=50%	R under MCR=60%	R under MCR=70%	R under MCR=80%	R under MCR=100%
Evaluation Mode							
MAPPO+IC3Net	10%	12.9	-39.1	-69.4	-97.6	-127.3	-208.4
MAPPO+G2A	7%	16.1	-26.8	-53.7	-84.5	-107.8	-192.8
MAPPO+ETCNet	16%	12.5	-20.4	-37.3	-58.4	-73.6	-236.4
MAPPO+NDQ	0%	13.3	6.4	4.8	2.7	0.3	-283.0
MAPPO+SchedIMAC	0%	12.0	7.5	5.6	4.9	3.8	-273.6
MAPPO+CGIBNet	17%	15.2	12.4	11.6	11.1	9.5	-265.3
Map	Medium						
Evaluation Mode	SCR	R under the left SCR	R under MCR=50%	R under MCR=60%	R under MCR=70%	R under MCR=80%	R under MCR=100%
MAPPO+IC3Net	21%	16.2	-93.5	-145.4	-227.1	-326.0	-533.4
MAPPO+G2A	18%	22.0	-72.2	-128.9	-187.4	-275.6	-541.6
MAPPO+ETCNet	30%	15.7	-42.5	-69.0	-122.5	-194.6	-554.7
MAPPO+NDQ	0%	2.5	-6.1	-10.5	-12.3	-16.6	-663.8
MAPPO+SchedIMAC	29%	14.5	8.8	5.9	2.6	-0.5	-609.8
MAPPO+CGIBNet	30%	19.8	16.6	15.8	13.5	11.8	-644.1
Map	Hard						
Evaluation Mode	SCR	R under the left SCR	R under MCR=50%	R under MCR=60%	R under MCR=70%	R under MCR=80%	R under MCR=100%
MAPPO+IC3Net	20%	-1254.0	-2064.1	-2223.1	-2527.2	-3001.5	-4638.3
MAPPO+G2A	19%	-1108.3	-1943.0	-2100.2	-2389.4	-2903.2	-3835.1
MAPPO+ETCNet	27%	-1387.9	-1744.3	-1948.7	-2188.8	-2473.7	-4842.5
MAPPO+NDQ	0%	-2529.6	-2684.2	-2750.7	-2824.6	-2895.2	-5934.0
MAPPO+SchedIMAC	27%	-1484.4	-1556.9	-1618.0	-1711.7	-1803.1	-5421.4
MAPPO+CGIBNet	28%	-1195.8	-1231.6	-1240.2	-1274.0	-1295.3	-6284.7

$r_{tot} = \sum_i^N (t \times r_{tp,i} + r_{cp,i} + r_{eb,i})$. The number of grids and cars on each map is consistent with Figure 5(b)-5(d).

Experimental setups. In this environment, we modify MAPPO [37] algorithm as the training framework and compare CGIBNet with various baselines, including IC3Net [18], G2A [17], SchedNet [19], ETCNet [20], NDQ [22] and IMAC [21], where IC3Net and G2A only schedule the edge connections in the communication graph while SchedNet and ETCNet explicitly constrains the redundant structural information. NDQ and IMAC only compress node information and ignore structural information. Since SchedNet and IMAC learn a scheduler in a similar way and they only consider one of structure compression or node compression, we combine these

two methods to construct a strong baseline, which is called SchedIMAC. For experimental hyperparameters, the training step is 3000(easy)/3000(medium)/10000(hard), the number of bits per message is 5, the discount factor is 0.99, the learning rate for actor/critic is 0.001/0.003, the batch size is 500, the optimizer is RMSprop, and all network backbones refer to MAPPO [37]. The particular hyperparameters of baselines mainly follow their original implementations. We first set the communication round of all methods to 1 for a fair comparison, because previous methods cannot reduce bandwidth occupancy in multi-round communication. The structural Lagrangian multiplier β_S and node Lagrangian multiplier β_X of our CGIBNet are set to 0.1 and 0.001 respectively.

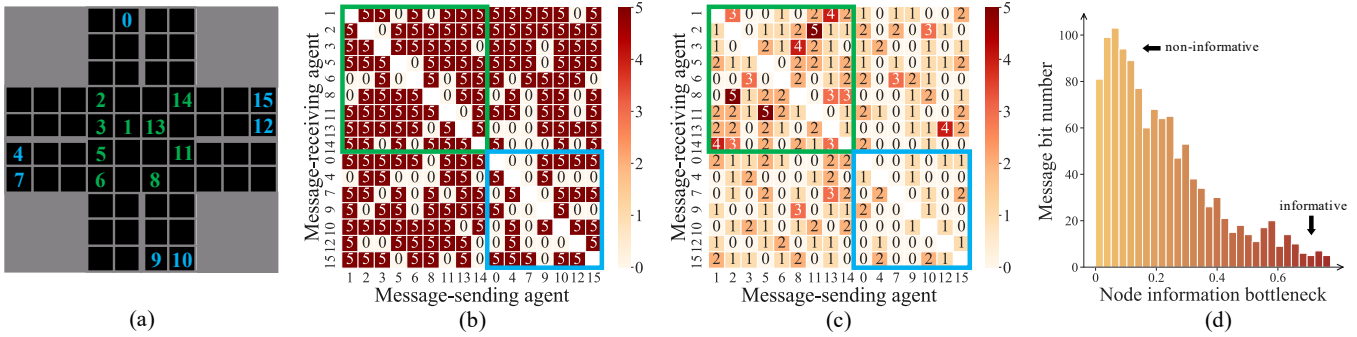


Fig. 6. Visualize the message transmission process. (a) Environment state. (b) Confusion matrix under SCR=28% (message bit is 5). (c) Confusion matrix under MCR=80%. (d) Node information bottleneck distribution of message bits.

Results. Table II shows the average results of 5 experiments on traffic control tasks. ‘R’ indicates cumulative reward per episode. The ‘SCR’ related results are obtained by standard evaluation without any restrictions, which indicates the ability of the corresponding model to compress the structure information in the communication graph. Specifically, SCR= $p\%$ in the table indicates that the available communication channels are compressed by $p\%$. The ‘MCR’ related results are obtained by limiting available message bits during the evaluation process, which ensures that the message compression strength of all methods is consistent so as to make a fair comparison. Specifically, MCR= $p\%$ in the table indicates that the available message bits are compressed by $p\%$.

According to the result of structural compression, NDQ is the only method to communicate using a fully connected graph (*i.e.*, SCR=0%) and it achieves poor performance on complex maps, which indicates traffic control tasks rely on scheduling with whom to communicate, otherwise too much redundant information will lead to multi-agent miscoordination. Interestingly, we find that the performance of CGIBNet is better than IC3Net even though CGIBNet has a larger SCR, which indicates our structural regularizer can effectively cut redundant edge connections in the communication graph. Additionally, ETCNet, SchedIMAC and CGIBNet are all explicitly structural compression methods with similar SCR on medium and hard maps, but the performance of CGIBNet is much better than that of ETCNet and SchedIMAC, which demonstrates the effectiveness of our method. Meanwhile, the suboptimal performance of SchedIMAC also verifies that combining existing methods (*i.e.*, SchedNet and IMAC) without a unified theoretical guide is not a good choice. Although G2A achieves the best performance thanks to its attention mechanism, it needs to occupy more bandwidth than CGIBNet.

According to the result of message compression, the performance of IC3Net, G2A and ETCNet has significantly reduced under MCR=50%~80%. This is because these methods do not compress the node information, thus a small number of bits cannot express sufficient content for communication. The performance of CGIBNet surpasses all other methods under MCR=50%~80% while maintaining a tolerable degradation compared to the standard evaluation, especially for the hard map. This indicates that CGIBNet can effectively determine

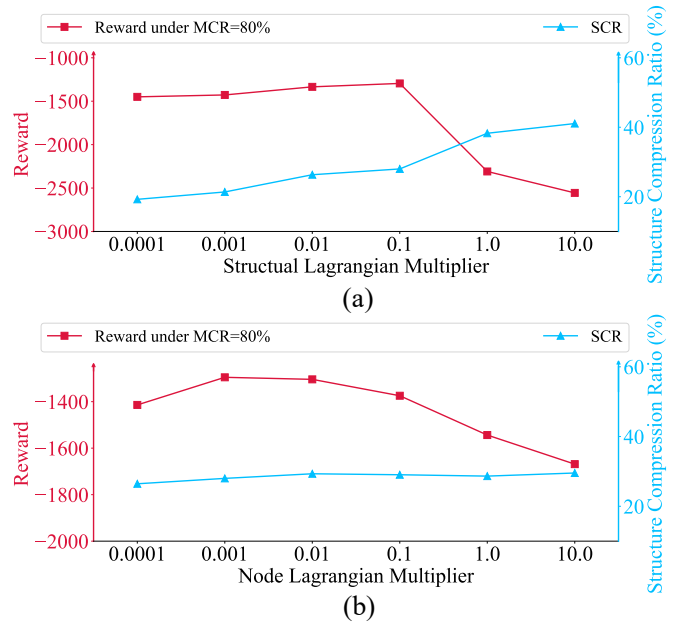


Fig. 7. The results on the hard map w.r.t. different Lagrangian multipliers β_S and β_X . (a) β_S ($\beta_X = 0.001$). (b) β_X ($\beta_S = 0.1$).

what messages to send and whom to address them so that just a few message bits are enough for communication. In addition, the performance of each method decreases drastically when all communication channels are closed (*i.e.*, MCR=100%), proving that the success of our method comes from the compressive communication graph instead of implicit coordination strategies are learned.

Visualize the message transmission process. As is shown in Figure 6, we visualize the communication confusion matrices and node information bottleneck distribution at a certain timestep on the hard map. Specifically, Figure 6(a) illustrates the environment state at one timestep. We can find the agents can be divided into two groups. One group is gathered at the intersection and highlighted in green, and another group is located at the entrance and highlighted in blue. Figure 6(b) shows the communication confusion matrix when only structure compression is considered (*i.e.*, SCR=28%), where

TABLE III
CGIBNET ON HARD MAP W.R.T. DIFFERENT COMMUNICATION ROUND. 22%/45% REPRESENTS THE SCR OF THE 1ST AND 2ND ROUNDS. MCR ONLY FOCUSES ON THE LAST ROUND.

Comm. round	SCR	R under the left SCR	R under MCR=50%	R under MCR=60%	R under MCR=70%	R under MCR=80%	R under MCR=100%
1	28%	-1195.8	-1231.6	-1240.2	-1274.0	-1295.3	-6284.7
2	22%/45%	-1073.2	-1092.1	-1106.8	-1127.4	-1158.3	-6586.5

TABLE IV
INFORMATION ON THE STARCRAFT II EVALUATION MAPS.

Map	Controlled ally units	Built-in enemy units	Action space \mathcal{A}	Observation space \mathcal{O}	State space \mathcal{S}
3b_vs_1h1m	3 Banelings	1 Hydralisk & 1 Medivac	8	37	52
1o2r_vs_4r	1 Overseer & 2 Roaches	4 Reapers	10	53	68
5z_vs_1ul	5 Zealots	1 Ultralisk	7	36	63
1o10b_vs_1r	1 Observer & 10 Banelings	1 Roach	11	85	148

the X-axis represents the ID of the message-sending agent, the Y-axis represents the ID of the message-receiving agent, and the value in the matrix represents the number of message bits. Figure 6(c) is similar to Figure 6(b), but the total message bits are compressed to 80% (*i.e.*, MCR=80%). From the results, we can find that a lot of message bits are transmitted between the agents at the intersection because they need to prevent collisions at this time (*i.e.*, the green box in Figure 6(b) and Figure 6(c)). On the contrary, the agents near the entrance are far apart and therefore communicate less with each other (*i.e.*, the blue box in Figure 6(b) and Figure 6(c)). The above shows that CGIBNet can effectively allocate communication resources in the large-scale multi-agent system. In addition, we also visualize the node information bottleneck distribution of message bits at this timestep. As is shown in Figure 6(d), the result indicates that our method can effectively compress the task-related information into a small number of message bits as discussed in ‘Drop message bits’ of Section IV-C.

The influence of β_S and β_X on CGIBNet. From the optimization perspective, Lagrangian multipliers β_S and β_X in (11) control the structure and node compression strength respectively. Figure 7 shows that as the compression strength increases (*i.e.*, β_S and β_X become larger), the performance of our model under MCR=80% will gradually rise. However, when they exceed a certain critical value, the information distortion caused by over-compression will lead to performance degradation or even collapse. *e.g.*, $\beta_S=1.0$ in Figure 7(a). Therefore, we recommend setting β_S to $10^{-2}\sim 10^{-1}$ and β_X to $10^{-3}\sim 10^{-2}$. Meanwhile, the monotonic relationship between β_S and SCR in Figure 7(a) further proves that β_S can effectively adjust the degree of structural compression in the communication graph.

Evaluate the multi-round communication. As discussed in Section II, all previous work about bandwidth-constrained communication cannot be extended to multiple rounds of communication, so we only evaluate our CGIBNet under this setting. Also, similar to some non-bandwidth limited communication methods [7], [10], we mainly focus on two-round communication. Three or more rounds of communication will lead to the training collapse, and we check there is

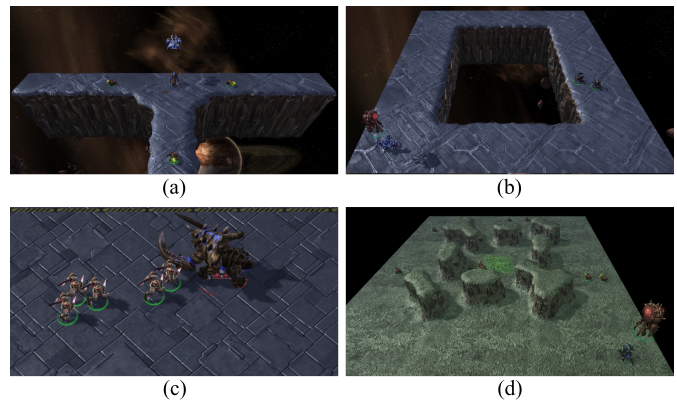


Fig. 8. StarCraft II evaluation maps. (a) 3b_vs_1h1m. (b) 1o2r_vs_4r. (c) 5z_vs_1ul. (d) 1o10b_vs_1r.

no MARL communication literature that reports such settings, which may be caused by the oversmoothness problem in the message passing. As is shown in Table III, our CGIBNet can obtain a multi-layer sparse communication graph through structure compression to reduce bandwidth occupation in each communication round. Specifically, in the two rounds of communication, the communication channels of the first and second rounds are compressed to 22% and 45%, respectively. Based on this sparse graph, we can further discard the message bits with less information in the last communication round to save bandwidth. *i.e.*, the result under MCR=50%~80%. More importantly, the performance of two-round communication is better than the single-round counterpart, showing our method can work well in the complex communication protocol.

C. StarCraft II

Environment description. StarCraft II micromanagement [51] is a real-time strategy game that is widely used in the MARL community [39]. Recently, Wang et al. [22] introduces four maps to explore the communication mechanism in value-based MARL frameworks. Specifically, these maps include 3b_vs_1h1m, 1o2r_vs_4r, 5z_vs_1ul and 1o10b_vs_1r, as is shown in Figure 8. The number and letter on the left of

TABLE V
EXPERIMENTAL RESULTS IN DIFFERENT RESTRICTIONS ON STARCRAFT II.

Map	3b_vs_1h1m						
Evaluation Mode	SCR	WR under the left SCR	WR under MCR=50%	WR under MCR=60%	WR under MCR=70%	WR under MCR=80%	WR under MCR=100%
QMIX+G2A	12%	74.8%	53.5%	46.0%	38.2%	29.4%	10.3%
QMIX+NDQ	0%	78.5%	72.4%	71.2%	69.8%	67.9%	2.9%
QMIX+IMAC*	0%	77.0%	71.8%	70.3%	68.4%	66.7%	2.4%
QMIX+CGIBNet	20%	78.1%	73.2%	72.0%	70.3%	69.2%	3.6%
Map	1o2r_vs_4r						
Evaluation Mode	SCR	WR under the left SCR	WR under MCR=50%	WR under MCR=60%	WR under MCR=70%	WR under MCR=80%	WR under MCR=100%
QMIX+G2A	15%	82.5%	54.8%	48.6%	43.3%	37.6%	18.5%
QMIX+NDQ	0%	81.6%	75.3%	73.8%	72.4%	71.7%	24.4%
QMIX+IMAC*	0%	81.0%	74.2%	73.0%	71.9%	70.2%	21.6%
QMIX+CGIBNet	26%	82.1%	78.0%	77.4%	77.0%	75.8%	17.7%
Map	5z_vs_1ul						
Evaluation Mode	SCR	WR under the left SCR	WR under MCR=50%	WR under MCR=60%	WR under MCR=70%	WR under MCR=80%	WR under MCR=100%
QMIX+G2A	21%	63.4%	36.9%	31.3%	25.6%	18.3%	22.0%
QMIX+NDQ	0%	62.5%	60.3%	58.4%	57.0%	55.8%	30.3%
QMIX+IMAC*	0%	61.6%	58.1%	56.7%	54.6%	52.4%	38.6%
QMIX+CGIBNet	37%	64.8%	63.7%	63.2%	62.4%	61.6%	33.6%
Map	1o10b_vs_1r						
Evaluation Mode	SCR	WR under the left SCR	WR under MCR=50%	WR under MCR=60%	WR under MCR=70%	WR under MCR=80%	WR under MCR=100%
QMIX+G2A	26%	84.3%	60.1%	53.2%	45.7%	37.8%	17.4%
QMIX+NDQ	0%	78.5%	74.9%	73.8%	72.1%	69.5%	10.6%
QMIX+IMAC*	0%	77.2%	70.6%	68.9%	66.4%	65.3%	7.8%
QMIX+CGIBNet	44%	83.8%	81.4%	80.3%	79.8%	78.7%	6.3%

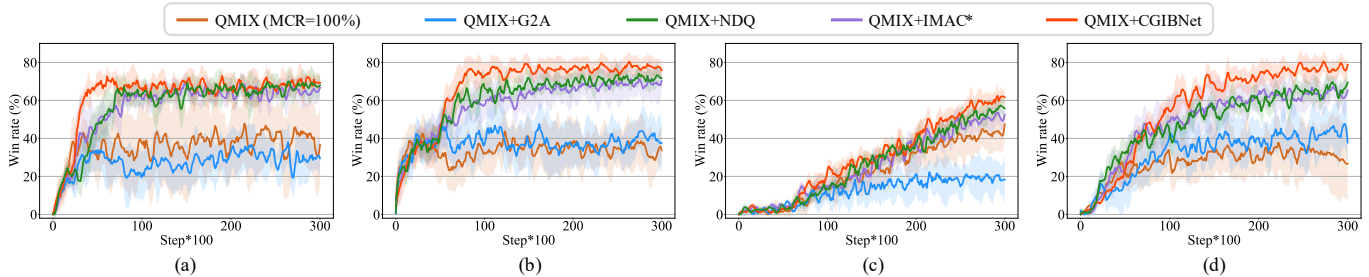


Fig. 9. The StarCraft II training curves under MCR=80%. (a) 3b_vs_1h1m. (b) 1o2r_vs_4r. (c) 5z_vs_1ul. (d) 1o10b_vs_1r.

‘vs’ indicate the number and type of agents we trained, and the right is the information of built-in agents. For the 3b_vs_1h1m map, 3 Banelings need to reach the designated location and attack the enemy at the same time. For 1o2r_vs_4r and 1o10b_vs_1r maps, 1 Overseer needs to continuously provide the enemy’s vision to guide the allied forces by communication. For the 5z_vs_1ul map, 5 Zealots need to cooperate and communicate frequently to defeat a powerful Ultralisk. We list key information for these maps in Table IV. It can be found that 1o10b_vs_1r is the most complex map.

Experimental setups. We choose QMIX [39], a well-known value-based method, as the training framework. Since IC3Net, SchedNet and ETCNet need to learn an additional actor as a scheduler, they are not suitable for extension into value-based frameworks. Therefore, we mainly compare

CGIBNet with G2A, NDQ and IMAC, where IMAC discards its actor-based scheduler (*i.e.*, not compatible with QMIX) and maintains the node compression part. This modified IMAC is denoted as IMAC*. For experimental hyperparameters, the training step is 30000, the learning rate is 0.001, the batch size is 64, the optimizer is Adam, and all network backbones refer to QMIX [39]. Other hyperparameters are consistent with traffic control experiments.

Results. Table V shows the average results of 5 experiments on StarCraft II, where ‘WR’ indicates the average win rate. For all maps, the conclusion is similar to that of traffic control. Specifically, CGIBNet can maximally reduce the communication channels between agents (*i.e.*, large SCR) and preserve sufficient information for decision-making. Also, it maintains its powerful ability under MCR=50%~80% set-

tings, especially for large-scale and complex multi-agent tasks, which verifies the superiority of our method under the value-based framework. Figure 9 demonstrates the curve of the win rate under MCR=80% during the training phase. We can find that CGIBNet converges faster on simple maps (*i.e.*, 3b_vs_1h1m and 1o2r_vs_4r) than its main competitors (*i.e.*, NDQ and IMAC*). We speculate that our method inherits the advantages of the IB theory [52], that is, the compact structure representation and node representation obtained by our method can improve the utilization of each sample. In addition, the poor performance of vanilla QMIX (*i.e.*, non-communication method) in Figure 9 verifies the necessity of communication on these four maps.

VI. CONCLUSION

In this article, we focus on how to learn a communication model to determine each agent is communicating what message and to whom in bandwidth-restricted settings. By modeling multi-agent communication as a directed complete graph, we propose our novel CGIBNet, which leverages the graph information bottleneck principle to compress the flow of node information over the graph structure while maximally preserves information for decision-making. We verify that CGIBNet is a universal module, which can be applied to various training frameworks and communication modes. Empirical results on Traffic Control and StarCraft II show the superiority of CGIBNet under bandwidth-restricted settings, especially for large-scale multi-agent systems.

REFERENCES

- [1] H. Wang and M. Li, "Model-free reinforcement learning for fully cooperative consensus problem of nonlinear multiagent systems," *IEEE Transactions on Neural Networks and Learning Systems*, 2020.
- [2] M. Li, Z. Cao, and Z. Li, "A reinforcement learning-based vehicle platoon control strategy for reducing energy consumption in traffic oscillations," *IEEE Transactions on Neural Networks and Learning Systems*, vol. 32, no. 12, pp. 5309–5322, 2021.
- [3] C. Sun, W. Liu, and L. Dong, "Reinforcement learning with task decomposition for cooperative multiagent systems," *IEEE transactions on neural networks and learning systems*, vol. 32, no. 5, pp. 2054–2065, 2020.
- [4] J. Chai, W. Li, Y. Zhu, D. Zhao, Z. Ma, K. Sun, and J. Ding, "Unmas: Multiagent reinforcement learning for unshaped cooperative scenarios," *IEEE Transactions on Neural Networks and Learning Systems*, 2021.
- [5] Q. Wei, Y. Li, J. Zhang, and F.-Y. Wang, "Vgn: Value decomposition with graph attention networks for multiagent reinforcement learning," *IEEE Transactions on Neural Networks and Learning Systems*, 2022.
- [6] Z. Zhang, D. Wang, and J. Gao, "Learning automata-based multiagent reinforcement learning for optimization of cooperative tasks," *IEEE transactions on neural networks and learning systems*, vol. 32, no. 10, pp. 4639–4652, 2020.
- [7] S. Sukhbaatar, R. Fergus *et al.*, "Learning multiagent communication with backpropagation," *Advances in neural information processing systems (NeurIPS)*, vol. 29, 2016.
- [8] J. Foerster, I. A. Assael, N. De Freitas, and S. Whiteson, "Learning to communicate with deep multi-agent reinforcement learning," *Advances in neural information processing systems (NeurIPS)*, vol. 29, 2016.
- [9] P. Peng and Y. Wen, "Multiagent bidirectionally-coordinated nets: Emergence of human-level coordination in learning to play starcraft combat games," *arXiv:1703.10069*, 2017.
- [10] A. Das, T. Gervet, J. Romoff, D. Batra, D. Parikh, M. Rabbat, and J. Pineau, "Tarmac: Targeted multi-agent communication," in *International Conference on Machine Learning (ICML)*. PMLR, 2019, pp. 1538–1546.
- [11] J. Jiang, C. Dun, T. Huang, and Z. Lu, "Graph convolutional reinforcement learning," in *International Conference on Learning Representations (ICLR)*, 2020.
- [12] E. Pesce and G. Montana, "Improving coordination in small-scale multi-agent deep reinforcement learning through memory-driven communication," *Machine Learning*, pp. 1–21, 2020.
- [13] M. Rangwala and R. Williams, "Learning multi-agent communication through structured attentive reasoning," *Advances in Neural Information Processing Systems (NeurIPS)*, vol. 33, pp. 10 088–10 098, 2020.
- [14] Y. Du, Y. Zhao, M. Fang, and J. Wang, "Learning predictive communication by imagination in networked system control," 2020.
- [15] W. Kim, J. Park, and Y. Sung, "Communication in multi-agent reinforcement learning: Intention sharing," in *International Conference on Learning Representations (ICLR)*, 2021.
- [16] S. Ahilan and P. Dayan, "Correcting experience replay for multi-agent communication," in *International Conference on Learning Representations (ICLR)*, 2021.
- [17] Y. Liu, W. Wang, Y. Hu, J. Hao, X. Chen, and Y. Gao, "Multi-agent game abstraction via graph attention neural network," in *Proceedings of the AAAI Conference on Artificial Intelligence (AAAI)*, vol. 34, no. 05, 2020, pp. 7211–7218.
- [18] A. Singh, T. Jain, and S. Sukhbaatar, "Learning when to communicate at scale in multiagent cooperative and competitive tasks," in *International Conference on Learning Representations (ICLR)*, 2018.
- [19] D. Kim, S. Moon, D. Hostallero, W. J. Kang, T. Lee, K. Son, and Y. Yi, "Learning to schedule communication in multi-agent reinforcement learning," in *International Conference on Learning Representations (ICLR)*, 2019.
- [20] G. Hu, Y. Zhu, D. Zhao, M. Zhao, and J. Hao, "Event-triggered communication network with limited-bandwidth constraint for multi-agent reinforcement learning," *IEEE Transactions on Neural Networks and Learning Systems*, 2021.
- [21] R. Wang, X. He, R. Yu, W. Qiu, B. An, and Z. Rabinovich, "Learning efficient multi-agent communication: An information bottleneck approach," in *International Conference on Machine Learning (ICML)*. PMLR, 2020, pp. 9908–9918.
- [22] T. Wang, J. Wang, C. Zheng, and C. Zhang, "Learning nearly decomposable value functions via communication minimization," in *International Conference on Learning Representations (ICLR)*, 2020.
- [23] P. Hernandez-Leal, B. Kartal, and M. E. Taylor, "A survey and critique of multiagent deep reinforcement learning," *Autonomous Agents and Multi-Agent Systems*, vol. 33, no. 6, pp. 750–797, 2019.
- [24] M. Zhang and Y. Chen, "Link prediction based on graph neural networks," *Advances in neural information processing systems (NeurIPS)*, vol. 31, 2018.
- [25] R. S. Sutton, D. A. McAllester, S. P. Singh, and Y. Mansour, "Policy gradient methods for reinforcement learning with function approximation," *Advances in Neural Information Processing Systems (NeurIPS)*, pp. 1057–1063, 2000.
- [26] Z. Huang, W. Xu, and K. Yu, "Bidirectional lstm-crf models for sequence tagging," *arXiv preprint arXiv:1508.01991*, 2015.
- [27] A. A. Alemi, I. Fischer, J. V. Dillon, and K. Murphy, "Deep variational information bottleneck," in *International Conference on Learning Representations (ICLR)*, 2017.
- [28] N. Tishby, F. C. Pereira, and W. Bialek, "The information bottleneck method," in *Proc. 37th Annual Allerton Conference on Communications, Control and Computing*, 1999, 1999.
- [29] X. B. Peng, A. Kanazawa, S. Toyer, P. Abbeel, and S. Levine, "Variational discriminator bottleneck: Improving imitation learning, inverse rl, and gans by constraining information flow," in *International Conference on Learning Representations (ICLR)*, 2018.
- [30] M. Igl, K. Ciosek, Y. Li, S. Tschitschek, C. Zhang, S. Devlin, and K. Hofmann, "Generalization in reinforcement learning with selective noise injection and information bottleneck," *Advances in neural information processing systems (NeurIPS)*, vol. 32, 2019.
- [31] K. Qian, Y. Zhang, S. Chang, M. Hasegawa-Johnson, and D. Cox, "Unsupervised speech decomposition via triple information bottleneck," in *International Conference on Machine Learning (ICML)*. PMLR, 2020, pp. 7836–7846.
- [32] T. Wu, H. Ren, P. Li, and J. Leskovec, "Graph information bottleneck," *Advances in Neural Information Processing Systems (NeurIPS)*, vol. 33, pp. 20 437–20 448, 2020.
- [33] C. Szegedy, W. Zaremba, and I. Sutskever, "Intriguing properties of neural networks," in *International Conference on Learning Representations (ICLR)*, 2014.
- [34] F. A. Oliehoek and C. Amato, *A concise introduction to decentralized POMDPs*. Springer, 2016.
- [35] J. Foerster, G. Farquhar, T. Afouras, N. Nardelli, and S. Whiteson, "Counterfactual multi-agent policy gradients," in *Proceedings of the AAAI conference on artificial intelligence (AAAI)*, vol. 32, no. 1, 2018.

- [36] J. K. Gupta and M. Egorov, “Cooperative multi-agent control using deep reinforcement learning,” in *International conference on autonomous agents and multiagent systems*. Springer, 2017, pp. 66–83.
- [37] C. Yu, A. Velu, E. Vinitzky, A. Bayen, and Y. Wu, “The surprising effectiveness of mappo in cooperative, multi-agent games,” *arXiv preprint arXiv:2103.01955*, 2021.
- [38] J. Schulman, F. Wolski, P. Dhariwal, A. Radford, and O. Klimov, “Proximal policy optimization algorithms,” *arXiv preprint arXiv:1707.06347*, 2017.
- [39] T. Rashid, M. Samvelyan, C. Schroeder, G. Farquhar, J. Foerster, and S. Whiteson, “Qmix: Monotonic value function factorisation for deep multi-agent reinforcement learning,” in *International Conference on Machine Learning (ICML)*. PMLR, 2018, pp. 4295–4304.
- [40] D. Ha, A. Dai, and Q. V. Le, “Hypernetworks,” *arXiv preprint arXiv:1609.09106*, 2016.
- [41] V. Mnih, K. Kavukcuoglu, D. Silver, A. Graves, I. Antonoglou, D. Wierstra, and M. Riedmiller, “Playing atari with deep reinforcement learning,” *arXiv preprint arXiv:1312.5602*, 2013.
- [42] J. Gilmer, S. S. Schoenholz, P. F. Riley, O. Vinyals, and G. E. Dahl, “Neural message passing for quantum chemistry,” in *International conference on machine learning (ICML)*. PMLR, 2017, pp. 1263–1272.
- [43] I. Csiszár, “I-divergence geometry of probability distributions and minimization problems,” *The annals of probability*, pp. 146–158, 1975.
- [44] E. Jang, S. Gu, and B. Poole, “Categorical reparameterization with gumbel-softmax,” in *International Conference on Learning Representations (ICLR)*, 2017.
- [45] D. P. Kingma and M. Welling, “Auto-encoding variational bayes,” in *International Conference on Learning Representations (ICLR)*, 2014.
- [46] R. A. Horn, “The hadamard product,” in *Proc. Symp. Appl. Math.*, vol. 40, 1990, pp. 87–169.
- [47] J. Chung, C. Gulcehre, K. Cho, and Y. Bengio, “Empirical evaluation of gated recurrent neural networks on sequence modeling,” *arXiv preprint arXiv:1412.3555*, 2014.
- [48] C. Dugas, Y. Bengio, F. Bélisle, C. Nadeau, and R. Garcia, “Incorporating functional knowledge in neural networks.” *Journal of Machine Learning Research (JMLR)*, vol. 10, no. 6, 2009.
- [49] D.-A. Clevert, T. Unterthiner, and S. Hochreiter, “Fast and accurate deep network learning by exponential linear units (elus),” *arXiv preprint arXiv:1511.07289*, 2015.
- [50] X. Glorot, A. Bordes, and Y. Bengio, “Deep sparse rectifier neural networks,” in *Proceedings of the fourteenth international conference on artificial intelligence and statistics*. JMLR Workshop and Conference Proceedings, 2011, pp. 315–323.
- [51] M. Samvelyan, T. Rashid, C. Schroeder de Witt, G. Farquhar, N. Nardelli, T. G. Rudner, C.-M. Hung, P. H. Torr, J. Foerster, and S. Whiteson, “The starcraft multi-agent challenge,” in *Proceedings of the 18th International Conference on Autonomous Agents and MultiAgent Systems (AAMAS)*, 2019, pp. 2186–2188.
- [52] O. Shamir, S. Sabato, and N. Tishby, “Learning and generalization with the information bottleneck,” *Theoretical Computer Science*, vol. 411, no. 29-30, pp. 2696–2711, 2010.



Baoxiang Wang received the B.E. degree from Shanghai Jiao Tong University, Shanghai, China, in 2014 and the Ph.D. degree from The Chinese University of Hong Kong, Hong Kong, China, in 2020, respectively.

He visited University of Alberta and Royal Bank of Canada for 16 months during his Ph.D.. He is currently an assistant professor in The Chinese University of Hong Kong, Shenzhen. The research interests of Baoxiang lie on reinforcement learning, online learning, and learning theory.



Furui Liu received the B.S. degree from Zhejiang University, Hangzhou, China, in 2015 and the Ph.D. degree from The Chinese University of Hong Kong, Hong Kong, China, in 2019, respectively.

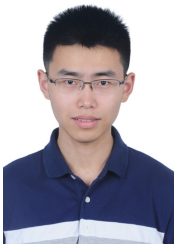
He was a visiting student at Max Planck Institute for Intelligent Systems, and Microsoft Research Asia. He is currently a senior researcher at Huawei Noah’s Ark Lab. His research interests include causal inference, deep learning and applications in large scale problems.



Fei Wu (Senior Member, IEEE) received the B.S. degree from Lanzhou University, Lanzhou, Gansu, China, the M.S. degree from Macao University, Taipa, Macau, and the Ph.D. degree from Zhejiang University, Hangzhou, China, in 1996, 1999, and 2002.

He was a Visiting Scholar with Prof. B. Yu’s Group, University of California at Berkeley, Berkeley, CA, USA, from 2009 to 2010. He is currently a Full Professor with the College of Computer Science and Technology, Zhejiang University. His

current research interests include machine learning, sparse representation, and multimedia retrieval.



Qi Tian received the B.S. degree from Chongqing University, Chongqing, China and the M.S. degree from Harbin Institute of Technology, Heilongjiang, China in 2017 and 2019, respectively. He is currently pursuing the Ph.D. degree with the College of Computer Science and Technology, Zhejiang University, Hangzhou, China, under the supervision of Prof. F. Wu and Assoc. Prof. K. Kuang.

His research interests include multi-agent reinforcement learning, machine learning, and adversarial learning.



Kun Kuang received his Ph.D. degree from Tsinghua University in 2019. He is now an Associate Professor in the College of Computer Science and Technology, Zhejiang University. He was a visiting scholar with Prof. Susan Athey’s Group at Stanford University. His main research interests include Causal Inference, Artificial Intelligence, Multi-agent Reinforcement Learning and Causally Regularized Machine Learning. He has published over 40 papers in major international journals and conferences, including SIGKDD, ICML, ACM MM, AAAI, IJCAI,

TNNLS, TKDE, TKDD, Engineering, and ICDM, etc.